PRAMANA
— journal of
physics

Vol. 66, No. 1
January 2006
pp. 295–304

Three-dimensional Ginzburg–Landau simulation of a vortex line displaced by a zigzag of pinning spheres

MAURO M DORIA[1,*], ANTONIO R DE C ROMAGUERA[1]
and WELLES A M MORGADO[2]
[1]Instituto de Física, Universidade Federal do Rio de Janeiro, C.P. 68528,
21941-972, Rio de Janeiro RJ, Brazil
[2]Instituto de Física, Pontifícia Universidade Católica do Rio de Janeiro,
C.P. 38071, 22452-970, Rio de Janeiro RJ, Brazil
[*]E-mail: mmd@if.ufrj.br

Abstract. A vortex line is shaped by a zigzag of pinning centers and we study here how far the stretched vortex line is able to follow this path. The pinning center is described by an insulating sphere of coherence length size such that in its surface the de Gennes boundary condition applies. We calculate the free energy density of this system in the framework of the Ginzburg–Landau theory and study the critical displacement beyond which the vortex line is detached from the pinning center.

Keywords. Ginzburg–Landau; tridimensional solution; pinning theory.

PACS Nos 74.80.-g, 74.25.-q, 74.20.De

1. Introduction

The basic idea of pinning theory is that the vortex is not rigid but adjustable to a local distribution of defects [1–3]. In this paper we consider a vortex line pinned by a zigzag of pinning centers that are insulating spheres of radius R of the order of the coherence length ξ. The boundary condition used by de Gennes [4] applies at the pinning sphere surface, considered as an insulator–superconductor interface. The straight line connecting these pinning centers is a path with abrupt right and left turns, whose zigzag fits into a single plane. As pointed out by Ovchinnikov [5], the investigation of various types of inclusions in superconducting materials is of particular interest because of the onset of metastable states. We have already considered a vortex depinning transition [6] similar to the one considered here which is being reviewed from the point of view of displaced defects.

An energetic balance makes the vortex line follow this zigzag path as long as trapping by the pinning spheres is advantageous as compared to the increase in length caused by the zigzag path. There is a critical path that sets a depinning

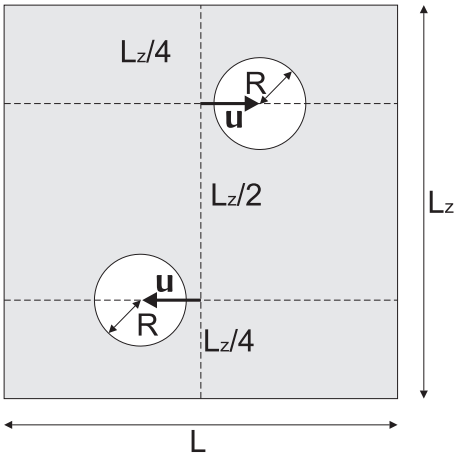

Figure 1. Schematic view of the unit cell middle plane. This view captures the displaced pinning spheres of radius R displaced by u along the x direction. The unit cell is orthorhombic with base side L and height L_z.

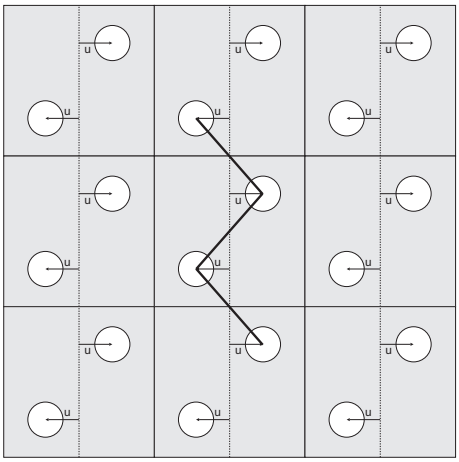

Figure 2. Nine equivalent unit cells are patched together here and the dark line connecting some pinning spheres shows the zigzag path followed by the vortex.

transition beyond which the stretched vortex line is no longer able to follow the zigzag path of the pinning centers.

This critical path is associated to a critical displacement u_c that we determine in this paper through numerical simulations of the Ginzburg–Landau theory [7]. From the point of view of this theory, pinning may be caused either by spatial fluctuations of the critical temperature, $T_c(\vec{x})$ [1], or by the mean free-path that changes the coefficient in front of the gradient term, $\xi(\vec{x})^2|(\vec{\nabla} - \frac{2\pi i}{\Phi_0}\vec{A})\Delta|^2$. The interaction between a vortex line and a pinning center has been considered by many authors in the context of the Ginzburg–Landau theory [8–11]. In this paper we consider only the no-magnetic shielding limit, such that the field penetrates in the superconductor and there is no Meissner effect. This situation can be viewed as a large κ limit, $\kappa = \lambda/\xi$ being the dimensionless Ginzburg–Landau parameter and λ the penetration depth.

The z-axis is the direction of the magnetic induction, and so, of the applied magnetic field, and perpendicular to it is the x-axis. In case of no defects, the vortex is a straight line oriented along the z-axis. The defects are equally spaced along the z-axis and assume alternate displacements u and $-u$ along the x-axis. Although the zigzag of defects fit into a single plane, the problem is genuinely three-dimensional because the defects are coherence length size spheres. Consider the position of two defects, $(L/2 - u, L/2, L_z/4)$ and $(L/2 + u, L/2, L_z/4)$. All others are obtained from these two forming an infinite lattice in the x, y and z directions. The position of all other defects can be obtained by translation of L along the x- or y-axis and by L_z along the z-axis. The periodicity due to the zigzag of defects allows one to describe this system through an orthorhombic unit cell of

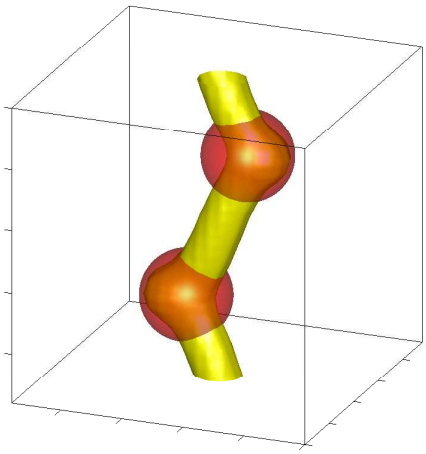

Figure 3. The vortex line remains pinned by the two displaced insulating spheres of radius $R = 1.8\xi$ in unit cell with $L = L_z = 12\xi$. The picture is the isosurface $|\Delta|^2 = 0.2507$, which means a density value approximately one fourth of its maximum value. The pinning spheres are shown in dark gray color.

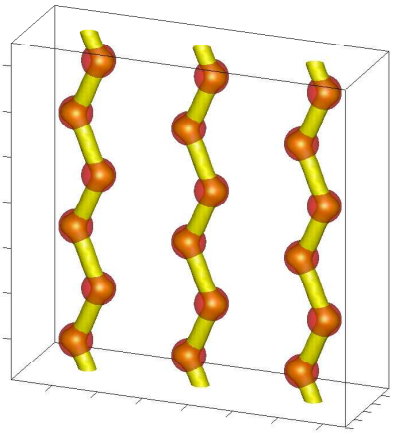

Figure 4. Nine equivalent unit cells are patched here displaying the vortex lines pinned by the spheres, as described in figure 3.

height L_z, and of square basis $L_x = L_y = L$, with two pinning centers inside, at the above positions $(L/2 - u, L/2, L_z/4)$ and $(L/2 + u, L/2, 3L_z/4)$ with respect to a coordinate frame whose origin is at the left-down corner of the unit cell. Figures 1 and 2 give a pictorial view of the geometrical arrangement of pinning centers inside the superconductor which is under investigation here.

The numerical results obtained from simulations of the Ginzburg–Landau theory yield the order parameter at each point of space. These results are visualized as isosurfaces of density, that is of the modulus of the order parameter squared, taken at a fixed value, as shown in figures 3 and 4. Notice that figure 4 corresponds to nine equivalent unit cells, as shown in figure 3, patched together. Many other possible pinned vortex configurations are possible in the pinning center arrangement displayed in figure 2. Figure 4 gives one among many others, but it is the only one described by the unit cell of figure 3. However these other possibilities are not considered here, although the present method is able to treat them by searching vortex configurations in larger unit cells containing several pairs of pinning centers. We restrict our study here to the minimum deviation of the vortex from the straight line, which is well-described by the present choice of unit cell. The present study involves some parameters related to the unit cell, L_z and L, and to the pinning center, u and R. The unit cell basis is fixed to $L = 12\xi$, and so our goal is to numerically obtain the Helmholtz free energy $F(u, L_z, R)$. For each point we obtain a density plot such as shown in figure 3. This paper is organized as follows. In §2,

we discuss our theoretical approach. In §3, we show the results obtained through numerical simulations and in §4, we summarize the main results of the work.

2. Theoretical approach

We find numerical solutions of the Ginzburg–Landau theory in the unit cell using a mesh grid to describe it [8–10]. The distance between two consecutive mesh points, a, is equal to 0.5ξ, consistent with the fact that a must be smaller than the coherence length ξ, which is the minimum physical scale of the Ginzburg–Landau theory. Thus the number of mesh points describing the unit cell square basis is P^2, and so $P = 25$ since $L = a(P-1)$. Notice that the pinning sphere also imposes a limit on the mesh parameter which cannot be larger than the pinning center radius, that is $a = 0.5\xi < R$. Otherwise there will be one or no mesh point describing the pinning region. In this case the order parameter does not vanish inside the defect but just undergoes a drop in its value. The energy density functional of the Ginzburg–Landau theory [7] is expressed in units of critical field energy density [10], $H_c^2/4\pi$ and the order parameter density, $|\Delta|^2$ is dimensionless, varying between 0 and 1. The concept of unit cell brings a periodicity to the problem, and so the search for the free energy minimum must be done under a constraint, the number of vortices inside the unit cell, $\vec{\nu}\phi_0$, described by integers: $\vec{\nu} = n_x\hat{x} + n_y\hat{y} + n_z\hat{z}$. The magnetic induction, which is the average of the local field taken over the unit cell volume, $\vec{B} = \int_v \vec{h}\mathrm{d}^3r/V$, has a relationship to these integers, and in reduced units is $\vec{B}(\vec{x}) = 2\pi\kappa\xi^2(n_x\hat{x}/L\cdot L_z + n_y\hat{y}/L\cdot L_z + n_z\hat{z}/L^2)$. In the present paper we only consider a single vortex oriented along the z-axis, hence $\vec{\nu} = \hat{z}$.

$$F = \int \frac{\mathrm{d}v}{V}\,\tau(\vec{x})\left[\xi^2\left|\left(\vec{\nabla} - \frac{2\pi i}{\Phi_0}\vec{A}\right)\Delta\right|^2 - |\Delta|^2\right] + \frac{1}{2}|\Delta|^4. \tag{1}$$

The function $\tau(\vec{x})$ is a step-like function used to describe the pinning spheres in this approach [10]. Explicitly we have $\tau(\vec{x}) = \tau_1(\vec{x})\tau_2(\vec{x})$ and

$$\tau_i(\vec{x}) = 1 - \frac{2}{1 + \mathrm{e}^{(|\vec{x}-\vec{x}_i|/R)^N}}, \tag{2}$$

where τ_i is equal to 0 inside and 1 outside the ith sphere. The above explicit representation of the τ function is necessary for computational reasons and for accuracy we take $N = 8$. In the limit $N \to \infty$, the function τ tends to the well-known Heaviside function, $\tau(\vec{x}) = \Theta\left(\frac{|\vec{x}-\vec{x}_1|}{R} - 1\right)\Theta\left(\frac{|\vec{x}-\vec{x}_2|}{R} - 1\right)$. The most significant advantage of the present method, is that the free energy functional, eq. (1) contains the appropriate boundary conditions to the problem. This removes the necessity of solving the theory in two independent regions and later applying the Neumann boundary conditions. Besides, the present method easily applies to internal regions of any shape, not just spherical, and finds its solution for the given normal–superconductor interface [10].

Since we are in the no-shielding limit, the vector potential $\vec{A}(\vec{x})$ is determined from the condition of magnetic flux quantization inside the unit cell. The vector

potential does not participate in the minimization process of the free energy density that only takes into account the real and imaginary parts of the order parameter. The free energy density contains two terms. The first term is the condensation energy density, $-\tau(\vec{x})\left|\Delta\right|^2+\frac{1}{2}\left|\Delta\right|^4$, which in the case of no vortices ($\left|\Delta\right|^2=1$) and no pinning sphere ($\tau=1$) has the value -0.5. The presence of a pinning sphere raises the energy since inside it the density vanishes ($\left|\Delta\right|^2=0$). And the second term, the kinetic energy density, is given by

$$\tau(\vec{x})\xi^2\left|\left(\vec{\nabla}-\frac{2\pi i}{\Phi_0}\vec{A}\right)\Delta\right|^2.$$

Notice that there is kinetic energy in the case of no vortices but with a defect. At the insulating–superconducting interface, τ changes from 1 to 0 and this causes a bending of the order parameter, which has some kinetic energy cost.

3. Results

The critical displacement $u_{\rm c}$ is better observed in the derivative of the kinetic energy density [6]. Figures 5 and 6 show the curves $\mathrm{d}F_{\rm kin}/\mathrm{d}u$ vs. u for two selected radii, namely $R=1.8\xi$, and $R=2.4\xi$, respectively, and in both cases a double hump structure with a local minimum between them is seen. For growing displacement u the first minimum of the kinetic energy density occurs for no displacement and the second minimum corresponds to the depinning transition $u_{\rm c}$. After the second hump there is a third minimum associated to the depinning from the second sphere. Thus detachment of the vortex from a pinning sphere makes the kinetic energy density reach a minimum. To understand this, consider the local maximum that precedes the detachment. For small u the vortex core is superposed to the two pinning centers. As long as the vortex is pinned by the two spheres, and follows the zigzag path, the order parameter has to adjust around one single common interface that involves both the vortex core and the pinning centers. The maximum stretch of

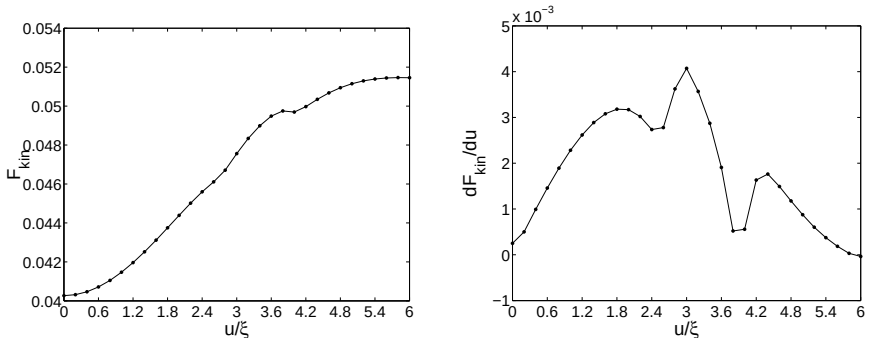

Figure 5. Kinetic energy and its derivative in the left and right part of the figure, respectively. The valleys in the derivative are associated to depinning. The critical displacement is associated to the minimum in these valleys. The pinning sphere radius is $R=1.8\xi$ and $L=L_z=12\xi$.

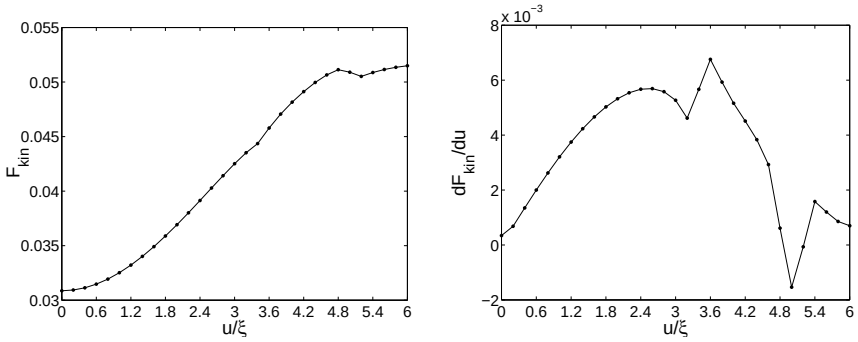

Figure 6. The kinetic energy and its derivative for a system with $R = 2.4\xi$, $L = L_z = 12\xi$ similar to figure 5. Thus the critical displacement depends on the radius of the defect.

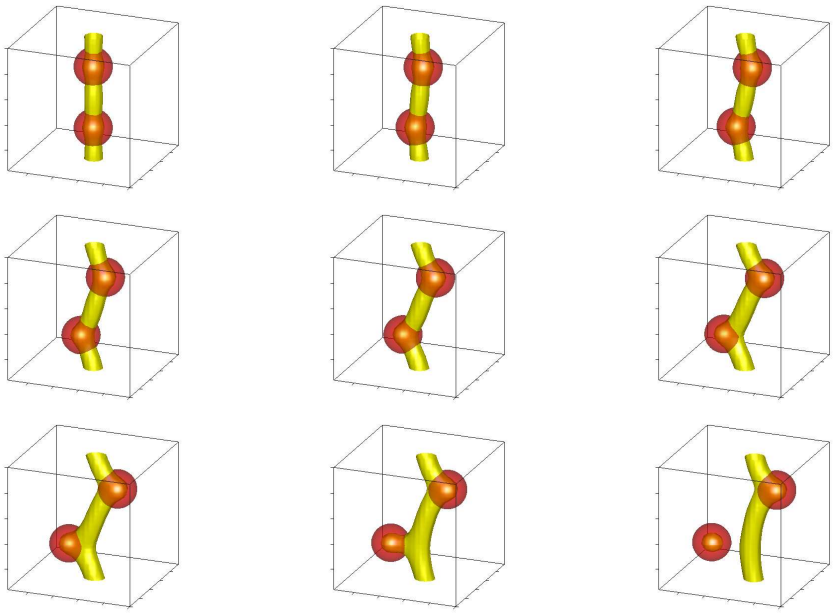

Figure 7. Sequence of views of the vortex line for several growing displacements u/ξ equal to 0.0, 0.4, 0.8, 1.2, 1.6, 2.0, 2.4, 2.8, and 3.2. The unit cell is cubic, $L_z = L = 12\xi$, and the pinning center is $R = 1.8\xi$. The isosurfaces are taken at a density approximately equal for all cases, namely, one fourth of its maximum value, $|\Delta|^2 \approx 0.25$.

the vortex line is the longest zigzag path, a configuration that demands maximum amount of circulating current around the vortex. Thus the maximum stretch of the vortex line is achieved when the kinetic energy reaches its maximum.

Beyond the maximum stretch the vortex unpins from one of the spheres, and the kinetic energy decreases for further displacement u. Consequently one expects that

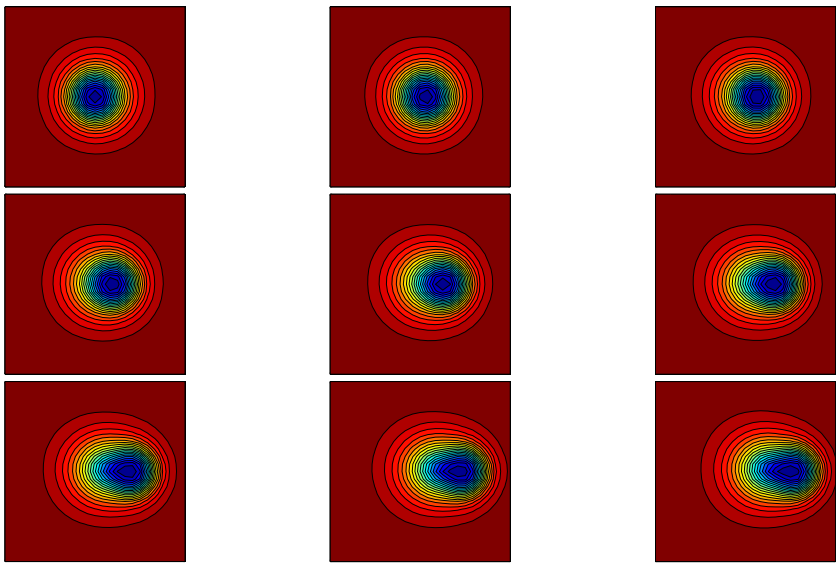

Figure 8. The same sequence of views of figure 7 is shown here through $z = 3L_z/4$ cuts of that unit cell ($L = L_z = 12\xi$, $R = 1.8\xi$). For the displacement $u = 3.2\xi$, the vortex line is still pinned by upper sphere.

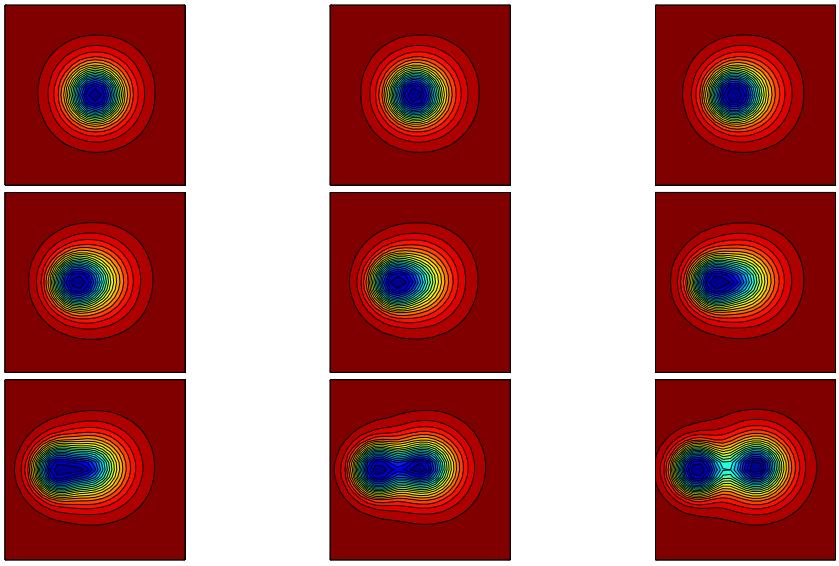

Figure 9. The same sequence of views of figure 7 is shown here through $z = L_z/4$ cuts of that unit cell ($L = L_z = 12\xi$, $R = 1.8\xi$). For the displacement $u = 3.2\xi$, the vortex line is detached from the lower sphere.

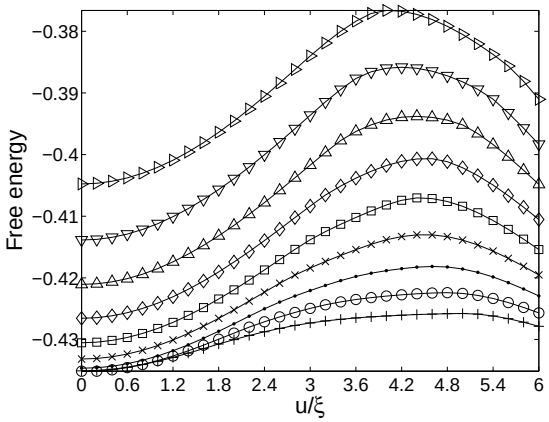

Figure 10. The free energy vs. the pinning sphere dislocation for different radii, all obtained for a cubic unit cell with $L_z = L = 12\xi$. The symbols $+$, $\circ$, $\bullet$, $\times$, $\square$, $\diamond$, $\triangle$, $\bigtriangledown$ and $\triangleright$ mean the radius R/ξ equal to 1.2, 1.4, 1.6, 1.8, 2.0, 2.2, 2.4, 2.6 and 2.8 respectively. The line of critical displacement u_c is also shown here. The vortex remains pinned to the zigzag of defects only for $u < u_c$.

the kinetic energy undergoes a minimum because following the detachment of the first pinning center from the vortex core the kinetic energy must rise again. Notice that in the case of nucleation of two independent surfaces from a single one, the deflection of the order parameter must be taken into account in each one of the new nucleated surfaces. This nucleation leads to an extra growth of the kinetic energy because there is a gradient of the order parameter in the interfaces. The total interface area has grown because there are two surfaces instead of just one after the nucleation. Here the two interfaces are the $z = L_z/4$ pinning sphere and the other one formed by the $z = 3L_z/4$ pinning center together with the vortex core. The depinning transition is shown in figure 7 that shows a sequence of increasing u displacements that lead to the depinning of the vortex line from the zigzag path. The same sequence is shown again through contour lines along the two planes that cross the pinning spheres in half, $3L_z/4$ (figure 8) and $z = L_z/4$ (figure 9).

The behavior of the free energy density vs. the displacement u is shown in figure 10 for several radii, ranging from $R = 1.2\xi$ to 2.8ξ, and for a cubic unit cell $L = L_z = 12\xi$. The left graphic in figure 12 exhibits the dependency of the critical displacement u_c on the radius of the spheres. Due to our choice of unit cell parameter L, R is limited to the interval $1.0\xi < R < 3.0\xi$, otherwise are smaller than the vortex core or the pinning spheres will not fit in the unit cell.

The critical displacement is dependent on the height of the unit cell L_z, as shown in figures 11 and in the right side of figure 12 for the case $R = 2.0\xi$. Figure 11 shows a set of free energy density curves vs. L_z associated to different u displacements in steps of 0.2ξ, ranging from 0 to 6.0ξ in the crescent sequence indicated therein. The zero displacement curve is the lowest in energy and the 6.0ξ is the largest, in agreement with the idea that large pinning centers increase the energy since they bring non-superconducting regions to the unit cell. The right side of figure 12 shows that unit cells with increasing L_z allow for larger critical displacements. The zigzag

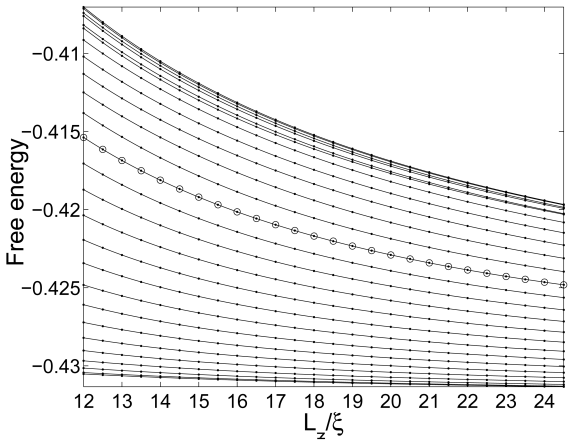

Figure 11. Several $F(u, Lz, R = 2.0\xi) \times Lz$ curves, associated to different u displacements, are shown here. The ascending values of u, ranging from 0.0 to 6.0ξ with a step of 0.2ξ, are shown such that the higher the value of u, the higher the free energy. For reference, the $u = 2.8\xi$ curve has its points magnified here.

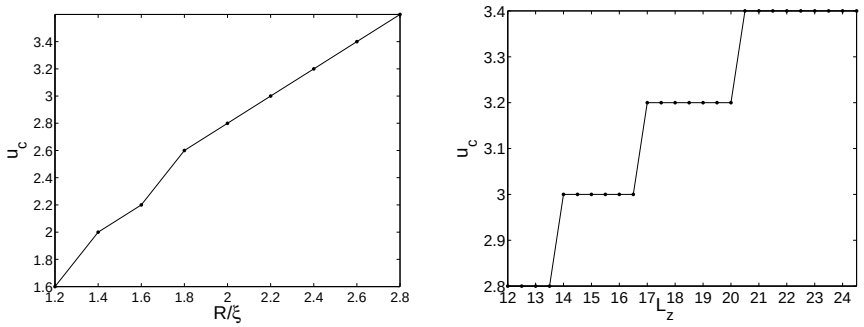

Figure 12. In the left side, the dependence of u_c on the radius of the sphere is shown ($L = L_z = 12\xi$). In the right side, the dependence of u_c on the height L_z is presented for a defect of radius $R = 2.0\xi$.

of pinning centers is not so demanding of the vortex line for large L_z, and so, we expect that large displacements are possible in these cases, as confirmed by figures 11 and 12.

4. Conclusions

The study of the interaction among pinning centers and vortices is crucial to the understanding of Type II superconductors. For this reason artificially made pinning centers are useful and many kinds have been fabricated [12–16] though not of the kind considered here. In this paper the Ginzburg–Landau theory was numerically

solved on a three-dimensional mesh to study properties of a vortex line near a zigzag of pinning centers. The pinning centers are insulating spheres of coherence length size and the system was described by an orthorhombic unit cell containing two displaced defects. We find that there is a critical displacement above which the vortex line is detached from a pinning center. Below this transition the vortex line is pinned by both defects and above by just one. The study of coherence length size defects may also be found useful in some other situations. Recently it has been shown that the nucleation of such defects is a mechanism to lower the energy of the superconducting state [17].

Acknowledgments

This research is supported in part by Instituto do Milênio de Nano-Ciências, CNPq, and FAPERJ (Brazil).

References

[1] A I Larkin, *Sov. Phys. JETP* **31**, 784 (1970)
[2] E H Brandt, *Rep. Prog. Phys.* **58**, 1465 (1995)
[3] J B Ketterson and S N Song, *Superconductivity*, 1st edn (Cambridge University Press, Cambridge, UK, 1999)
[4] P G de Gennes, *Superconductivity in metals and alloys*, 2nd edn (Persus Book, Massachusetts, 1989)
[5] Yu N Ovchinnikov, *Sov. Phys. JETP* **52**, 755 (1980); **57**, 1162 (1982); **57**, 136 (1983)
[6] Antonio R de C Romaguera and M M Doria, *Euro. Phys. J.* **B42**, 3 (2004)
[7] A A Abrikosov, *Sov. Phys.* **5**, 1174 (1957)
[8] M M Doria and Sarah C B Andrade, *Phys. Rev.* **B60**, 13164 (1999)
[9] M M Doria and Gilney F Zebende, *Braz. J. Phys.* **32**, 690 (2002)
[10] M M Doria and Gilney F Zebende, *Phys. Rev.* **B66**, 064519 (2002)
[11] D J Priour and H A Fertig, *Phys. Rev.* **B67**, 054504 (2003)
[12] A Bezryadin and B Pannetier, *J. Low Temp. Phys.* **98**, 251 (1995)
[13] J Y Lin, M Gurvitch, S K Tolpygo, A Bourdillon, S Y Hou and Julia M Phillips, *Phys. Rev.* **B54**, R12717 (1996)
[14] V V Moshchalkov, M Baert, V V Metlusko, E Rossell, M J Van Bael, K Temst and Y Bruynserade, *Phys. Rev.* **B57**, 3615 (1998)
[15] V Yurchenko, P Lahl, S Bunte, M Jirsa and R Wordenweber, *Physica* **C404**, 426 (2004)
[16] W V Pogosov and V V Moshchalkov, *Physica* **C404**, 285 (2004)
[17] M M Doria and Antonio R de C Romaguera, *Euro. Phys. Lett.* **67**, 446 (2004)